

000 001 002 003 004 005 006 007 008 FROM REST TO ACTION: ADAPTIVE WEIGHT 009 GENERATION FOR MOTOR IMAGERY CLASSI- 010 FICATION FROM RESTING-STATE EEG USING 011 HYPERNETWORKS 012 013

014 **Anonymous authors**
 015 Paper under double-blind review
 016
 017
 018
 019
 020
 021
 022
 023
 024
 025
 026
 027
 028
 029
 030
 031

ABSTRACT

032 Existing EEG-based brain-computer interface (BCI) systems require long calibra-
 033 tion sessions from the intended users to train the models, limiting their use in real-
 034 world applications. Additionally, despite containing user-specific information and
 035 features correlating with BCI performance of a user, resting-state EEG data is un-
 036 derutilized, especially in motor imagery decoding tasks. To address the challenge
 037 of within and across-user generalisation, we propose a novel architecture, Hyper-
 038 EEGNet, which integrates HyperNetworks (HNs) with the EEGNet architecture
 039 to adaptively generate weights for motor imagery classification based on resting-
 040 state data. Our approach performs similarly in a Leave-Subject-Out scenario using
 041 a dataset with 9 participants, compared to the baseline EEGNet. When the dataset
 042 size is scaled, with 33 participants' datasets, the model demonstrates its generali-
 043 sation capabilities using the information from resting state EEG data, particularly
 044 when faced with unseen subjects. Our model can learn robust representations in
 045 both cross-session and cross-user scenarios, opening a novel premise to leverage
 046 the resting state data for downstream tasks like motor imagery classification. The
 047 findings also demonstrate that such models with smaller footprints reduce mem-
 048 ory and storage requirements for edge computing. The approach opens up avenues
 049 for faster user calibration and better feasibility of edge computing, a favourable
 050 combination to push forward the efforts to bring BCIs to real-world applications.
 051

1 INTRODUCTION

052 The growing use of electroencephalograms (EEGs) in brain-computer interfaces (BCIs) has gained
 053 attention due to their non-invasive nature and high temporal resolution, making them ideal for de-
 054 coding brain activity patterns in real-time (Schalk et al., 2024). BCIs, providing an interface between
 055 the brain and external devices, have applications in neurorehabilitation, assistive technologies, and
 056 neuroprosthetics. Among the various paradigms within BCIs, motor imagery (MI) decoding, which
 057 involves classifying imagined movements by the users from EEG signals, is of greater interest for
 058 decoding motor control. However, despite advances in hardware and software pipelines, MI-based
 059 BCIs have substantial challenges to bring them to real-world applications for generalised usage. The
 060 challenges with non-invasive BCIs are particularly in achieving robust and consistent performance
 061 across users and sessions (Saha & Baumert, 2020).

062 An outstanding challenge in MI-BCI systems is the variability in brain signals across users and
 063 sessions. This variability arises from differences in individual neural patterns, low signal-to-noise
 064 ratio, and varying conditions of the users, like fatigue or attention (Pan et al., 2022; Kobler et al.,
 065 2022). These differences cause inconsistencies in decoding MI patterns, limiting the generalizability
 066 of BCIs in real-world applications. The ability to generalize across users and sessions is necessary
 067 for practical and accessible applications of BCIs, especially in scenarios where collecting large
 068 amounts of personalized data is unfeasible.

069 In addition to cross-user variability, BCI performance is also hindered by BCI illiteracy (Allison
 070 & Neuper, 2010), where certain individuals cannot generate the neural signals necessary for BCI

control. Though the concept of BCI illiteracy has been debated and its cause is a subject of research (Becker et al., 2022; Thompson, 2019; Alonso-Valerdi & Mercado-García, 2021), the result is evident across datasets. This makes designing universally effective BCIs challenging. Research has also focused on the predictors of BCI performance, helping to pre-identify individuals who may face difficulties with BCIs, which may guide personalized interventions or optimizations. Importantly, much of the research has used resting-state EEG data to develop these predictors (Tzdaka et al., 2020; Trocellier et al., 2024; Blankertz et al., 2010). Resting-state data, collected while the user is relaxed, offers insights into baseline brain activity without task-specific requirements, making it an attractive candidate for predicting BCI proficiency. Moreover, resting state EEG data is also a marker for user identification (Ma, 2015; Choi et al., 2018; Wang et al., 2019), depicting user-specific information.

Data-driven deep-learning models have effectively improved BCI performance on different tasks (Hossain et al., 2023; Tibrewal et al., 2022). Transfer learning, where models trained on data from one individual or group can be adapted to another, holds promise for creating systems that work across different users, including able-bodied and SCI patients (Nagarajan et al., 2024; Xu et al., 2021). Furthermore, a study by Camille Benaroch & Lotte (2022) has used user-specific frequencies to optimize decoding algorithms, applying data-driven approaches. However, to our knowledge, this is the first work to use resting state EEG data to train the model for motor-imagery classification. The major contributions of this work are as follows:

- Propose a novel HyperEEGNet architecture using HyperNetworks to learn unique user-specific representations as adaptive weights for the underlying task in EEG decoding.
- Demonstrate the significance of resting state EEG data to solve downstream tasks like motor imagery classification using data-driven learning.

2 METHOD

2.1 DATASETS

The dataset used in this study consists of electroencephalogram (EEG) recordings from 87 individuals who participated in motor imagery (MI) tasks and resting-state conditions Dreyer et al. (2023). The dataset is unique, given the large number of participants and the available recordings for each user. The EEG data were collected using 27 electrodes placed with a 10-20 configuration system, each sampling at a rate of 512 Hz. The dataset consisted of 70 hours of recordings of 8-second long runs when participants performed motor imagery, i.e. imagining left and right-hand movements following a visual cue on the screen.

This work used the sub-dataset "A" with 60 participants. The dataset mentions that 18 participants reported having noisy channel data or distractions from the environment during the sessions. These participants are ignored in the study. The dataset has two runs for each participant, which were used for training the model, while the rest of the four runs are termed "online" runs. Following the benchmark set by Dreyer et al. Dreyer et al. (2023), each participant's two "acquisition" runs are used for training, and the four online runs are used as test sets for the within-user across-session scenario. For the across-user scenario, data from the last 9 participants (20%) was considered a test set, while the rest of the data from the 33 participants was used for training. A band-pass filter with a frequency range of 0.5-40 Hz was used to prepare the raw EEG data for analysis. Epochs, or time segments of EEG data, were created by segmenting the 3 seconds of data following the event marker at the onset of the visual cue for movement imagination. The resting state data was extracted from the first two seconds of the trial, where the participants focused on a fixation cue and were not explicitly instructed to rest.

To understand the effectiveness of the proposed approach on a comparatively smaller dataset with 9 participants, BNCI 2014 IIa Competition Dataset Brunner et al. (2008) is used. The dataset consists of electroencephalogram (EEG) signals from 9 individuals who participated in motor imagery (MI) tasks and resting state conditions. The EEG data were collected using 22 electrodes, each sampling at a frequency of 250 Hz. The analysis involved two classes: right-hand and left-hand movement imagery, while feet and tongue movements were ignored. Each epoch consisted of 4 second-long motor imagery activity. The resting state data was extracted from the first two seconds of the trial, where the participants focused on a fixation cue and were not explicitly instructed to rest.

108
109

2.2 RESTING STATE CONNECTIVITY ANALYSIS

110
111
112
113
114
115
116
117

The resting state analysis for both datasets was common. The preprocessing phase for the analysis involved using MNE-Python Gramfort et al. (2013) to process resting-state EEG data from each epoch spanning a time window from 0 to 2 seconds relative to the trial start onset. A continuous wavelet transform (CWT) using Morlet wavelets Tallon-Baudry et al. (1997) was then applied to decompose the EEG signals into these desired frequency bands: theta (4–8 Hz), alpha (8–13 Hz), and beta (13–30 Hz). To analyze steady-state connectivity patterns from resting-state EEG data, we employed spectral connectivity measures, including coherence (COH) and phase-locking value (PLV) Lachaux et al. (1999).

118
119

Spectral connectivity was estimated using Coherence (COH) and phase-locking value (PLV) as connectivity metrics to evaluate both amplitude and phase coupling between different brain regions.

120
121

Coherence measures the linear relationship between two signals in the frequency domain, capturing both the amplitude and phase coupling across frequency bands.

122
123
124

$$COH(f) = \frac{|E[S_{xy}(f)]|}{\sqrt{E[S_{xx}(f)] \cdot E[S_{yy}(f)]}} \quad (1)$$

125
126
127
128

The cross-spectrum $S_{xy}(f)$ is a measure of the spectral density of the correlation between two signals $x(t)$ and $y(t)$ at a specific frequency f . The auto-spectra $S_{xx}(f)$ and $S_{yy}(f)$ are the Fourier transforms of the autocorrelation functions of $x(t)$ and $y(t)$, respectively, and represent the power spectral densities of the signals.

129
130
131
132

Similarly, Phase-Locking Value (PLV) measures the consistency of the phase difference between two signals across multiple trials, independent of their amplitude. PLV ranges from 0 to 1, where 0 indicates no phase locking (random phase differences) and 1 indicates perfect phase synchronization (constant phase difference).

133
134
135

$$PLV = \left| E \left[\frac{S_{xy}(f)}{|S_{xy}(f)|} \right] \right| \quad (2)$$

136
137
138

The resting state EEG analysis described above was performed on the segmented two-second-long time window from EEG data, and the resulting connectivity matrices were averaged across each participant trial to obtain a representation of functional connectivity.

139

2.3 MODEL ARCHITECTURE AND TRAINING

140
141
142
143
144
145
146

This study proposes a novel architecture that combines the feature extraction capabilities of EEGNet (Lawhern et al., 2018) with the adaptability of HyperNetworks (Ha et al., 2017) for motor imagery classification. This method uses a hypernetwork to generate adaptive weights for EEGNet, leveraging user-specific information from the resting state EEG data for cross-session and cross-user generalisation. Figure 1 depicts the model architecture and the learning mechanism.

147
148

2.3.1 EEGNET

149
150
151
152
153
154

EEGNet is a specialized neural network architecture designed to handle the unique characteristics of EEG signals. The model includes temporal and spatial convolutional layers optimized to capture relevant patterns from the multi-channel EEG data. Temporal convolutional layers focus on identifying patterns within the time domain of the signals, while spatial convolutional layers extract information based on the relationships between different EEG channels (Tshukahara, 2021). The EEGNet model was implemented using the Torcheeg framework (Zhang et al., 2024).

155
156

2.3.2 HYPERNETWORK

157
158
159
160
161

Hypernetworks are neural networks that generate the weights for another network (the main network: EEGNet) instead of learning them directly. For this study, the designed hypernetwork generated the weights of the core layers (conv2d and linear layers) of EEGNet. The hypernetwork (HyperNet) is a fully connected neural network with hidden layers of sizes 256 and 512, followed by a dropout with a probability of 0.3 to improve generalization. The resting state EEG data extracted from the two-second long time window are the inputs to this hypernetwork.

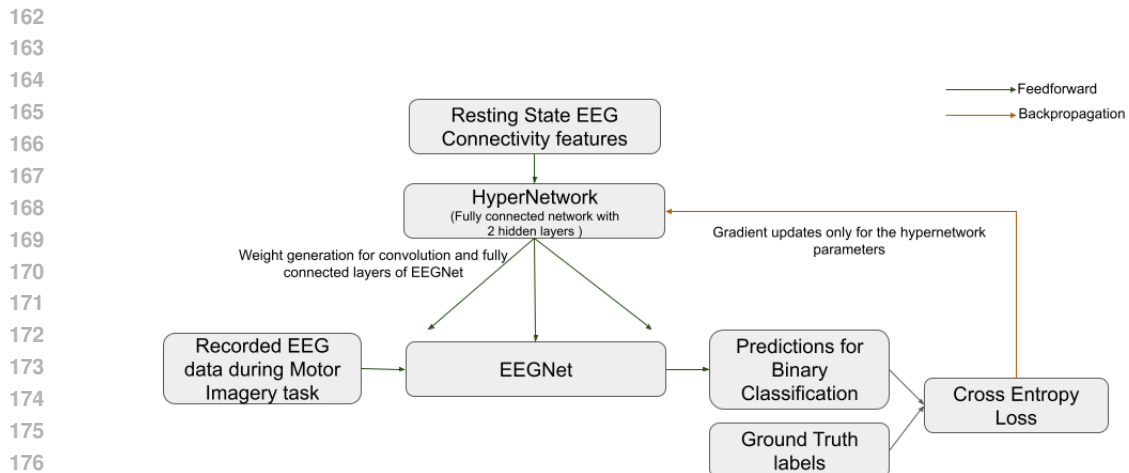


Figure 1: Overview of the proposed HyperEEGNet learning mechanism.

2.3.3 HYPEREEGNET TRAINING

The combined architecture, including the HyperNet and EEGNet, is trained as follows:

- HyperNet is used as a feedforward network to generate weights for EEGNet using resting-state connectivity data with dropout.
- Motor imagery activity data is extracted from a predefined time window (based on the experimental paradigm) in the raw data to perform the binary class classification with a forward pass on EEGNet with the generated weights from HyperNet.
- Cross entropy loss is accumulated for a batch of 50 epochs, and backpropagation is performed only on HyperNet parameters. Adam optimiser with learning rate 1e-4 is used.

2.4 EXPERIMENTAL SETUP AND PERFORMANCE EVALUATION

The experiment is set to evaluate two conditions: cross-session and cross-user for each dataset: BCI IV IIa and Dreyer et al. (2023) with a baseline comparison with EEGNet. The experiments were performed using the dataset from MOABB library (Aristimunha et al., 2023), and models were trained and evaluated using Torch and sci-kit-learn libraries.

2.4.1 CROSS-SESSION CONDITION

For the dataset from Dreyer et al. (2023), the "acquisition runs" from 33 participants are used for training and stratified 5-fold cross-validation is used to select the best model. Performance evaluation with accuracy metrics is performed for the "online" runs to evaluate HyperEEGNet compared to EEGNet.

For the BCI IV IIa dataset, the data from all nine participants is divided into five folds with stratified cross-validation; each fold in the iteration is considered as a test set while the other set is split with an 80-20 ratio to choose the best-performing model on the validation set. Accuracy metrics on the test set are evaluated for HyperEEGNet and compared with EEGNet.

2.4.2 CROSS-USER CONDITION

For the Leave-N-out (with N=8,16 and 32) strategy to test the HyperEEGNet performance compared to EEGNet, the "acquisition runs" from randomly selected (42-N) participants were used for training. 20% split is used as a validation set to select the best model. Performance evaluation with accuracy metrics is performed using data from the N participants for the "online" runs to evaluate HyperEEGNet compared to EEGNet. Analysis of such 100 random combinations reports the mean accuracy and standard deviation in Table 4 in the Appendix section. Non-parametric statistical tests

(Wilcoxon Signed Rank Test) recorded a statistically significant increase ($p < 0.005$ for all N) in the performance using HyperEEGNet compared to EEGNet.

3 RESULTS

The results of the experiments, as presented in Table 1, report the performance of the proposed HyperEEGNet architecture compared to the baseline EEGNet in cross-session conditions on the Dreyer et al. (2023) dataset. For the cross-session condition, the HyperEEGNet again outperformed EEGNet, with a mean accuracy of $83.51\% \pm 0.68$ compared to EEGNet's $75.87\% \pm 6.62$.

Iteration	Cross-Session Condition	
	HyperNet + EEGNet (%)	EEGNet (%)
1	84.25	81.49
2	83.47	73.79
3	83.78	65.46
4	83.66	81.26
5	83.51	77.35
Mean \pm SD	83.51 ± 0.68	75.87 ± 6.62

Table 1: Mean accuracy with standard deviation (SD) across five iterations of cross-session (on online runs) conditions on Dreyer et al. (2023) Dataset .

Participant ID	HyperNet + EEGNet (%)	EEGNet (%)
1	60.07	83.33
2	53.47	62.85
3	63.89	82.29
4	76.04	58.68
5	59.03	54.17
6	68.40	72.22
7	68.40	63.54
8	75.00	88.19
9	64.58	70.83
Mean \pm SD	65.43 ± 07.40	70.68 ± 11.90

Table 2: Mean accuracy with standard deviation (SD) across five iterations of cross-user condition on BCI Competition IV IIa Dataset with Leave One Subject Out (LOSO) strategy.

Iteration	HyperNet + EEGNet (%)	EEGNet (%)
1	79.61	79.38
2	82.21	81.70
3	80.69	80.12
4	79.61	81.27
5	79.18	80.31
Mean \pm SD	80.26 ± 1.23	80.56 ± 00.93

Table 3: Mean accuracy with standard deviation (SD) across five iterations of cross-session (using all 9 participants' data) condition for BCI Competition IV IIa Dataset.

The HyperEEGNet and baseline EEGNet models were evaluated using the Leave-One-Subject-Out (LOSO) strategy on the BCI Competition IV IIa dataset. The results represented in Table 2 indicate that while EEGNet achieved a higher overall mean accuracy ($70.68\% \pm 11.90$) compared to HyperEEGNet ($65.43\% \pm 07.40$), there were notable differences in performance for certain participants. For instance, HyperEEGNet outperformed EEGNet for Participant IDs 4, 5, and 7, with improvements of 17.36%, 4.86%, and 4.86%, respectively. However, for participants with higher

270 baseline performance (e.g., Participant IDs 1, 3, and 8), EEGNet achieved superior results. For the
 271 cross-session evaluation, the performance of HyperEEGNet and EEGNet was more comparable, as
 272 observed in Table 3, with mean accuracies of $80.26\% \pm 1.23$ for HyperEEGNet and $80.56\% \pm 0.93$
 273 for EEGNet.

274

275

276 4 DISCUSSION

277

278 4.1 LEARNING REPRESENTATIONS FROM RESTING STATE

279

280 Experimental results indicate the unique possibility of leveraging resting state EEG data for learning
 281 downstream tasks like motor imagery classification. The comparison across two different sizes of
 282 datasets also confirms the positive outcomes of the efforts in the field to build large, robust datasets
 283 for training foundational models (Ferrante et al., 2024; Chen et al., 2024). During the training phase
 284 for HyperEEGNet architecture on the Dreyer et al. 2023 dataset, we also observed a steep learning
 285 curve, indicating a rapid convergence in 50 epochs. The HyperNet was also prone to overfitting with
 286 a larger epoch size (500+) for training, especially in the case of cross-user conditions, where it was
 287 more evident. Notably, the smaller standard deviation for HyperEEGNet across the performance
 288 benchmarks indicates more stable performance across subjects than EEGNet.

289

290 Though the proposed approach focused on learning the adaptive weights for two class motor imagery
 291 classification, it opens up a future direction to generalise the learning mechanism across different
 292 downstream tasks or a larger number of classes for motor imagery.

293

294 4.2 INTERPRETING HYPEREEGNET

295

296 Apart from the performance metrics, some takeaways indicate potential as well as raise interesting
 297 questions in learning via the proposed approach. There are participants from both datasets known to
 298 have lower BCI performance across studies using different classifiers, and the contrary is true where
 299 few participants have consistently higher accuracies when trained specifically on the participant’s
 300 data. For example, Participant ID 4 in the BCI Competition dataset has low BCI performance. How-
 301 ever, Participant ID 3 has consistently high accuracies when using different classifiers. Surprisingly,
 302 the proposed approach performs well on Participant IDs 4, 5, and 7 but doesn’t do well enough for
 303 Participant ID 3 in cross-user scenarios. These questions are open for exploration since they need
 304 to interpret the weights generated by the HyperNet; how do they compare with an EEGNet trained
 305 directly on activity data? Moreover, the resting state data can be represented in many ways; the
 306 proposed work did not explore optimising the representations for resting-state brain connectivity.
 307 There could be other important features useful for downstream tasks that are not captured in the
 308 connectivity measures.

309

310 4.3 TRANSFER LEARNING AND FEW-SHOT LEARNING

311

312 While the current approach can be considered an approach towards meta-learning by learning to
 313 learn weights of the downstream task, the work has not explored the paradigm of few-shot learning
 314 for faster adaptation compared to other existing approaches or the efficacy of this architecture com-
 315 pared with other transfer learning approaches. A benchmark against approaches for transfer learning
 316 and few-shot learning successful on EEG datasets is necessary to justify the approach holistically.

317

318 4.4 HYPERNETS FOR SMALLER FOOTPRINTS

319

320 Current work focused on successfully learning representations from resting state EEG data for mo-
 321 tor imagery without optimising the size of the HyperNet. However, hypernetwork architectures
 322 are helpful for model compression. Efforts towards model compression without an impact on per-
 323 formance can be fruitful for real-world deployment of the BCI models. Task-specific information
 324 like restricting the input frequency bands and identifying efficient connectivity metrics can be an
 325 interesting future direction.

324 **5 CONCLUSION**

325

326 This work propose a novel HyperEEGNet architecture and introduces a promising new direction in
 327 EEG-based brain-computer interfaces (BCIs) by leveraging HyperNetworks to adaptively generate
 328 weights for EEGNet, utilizing resting-state EEG data for downstream motor imagery classification.
 329 This approach underscores the untapped potential of resting-state EEG, not only as a passive baseline
 330 to evaluate or correlate the BCI performance or illiteracy but as a source of user-specific features
 331 that enhance generalization across subjects and sessions. The positive results across cross-user and
 332 cross-session conditions indicate that resting-state data can be effectively harnessed for learning
 333 personalized representations in BCIs.

334 With focused efforts, instead of relying solely on task-related data, using resting-state data for model
 335 training can reduce the need for large amounts of labelled task data, which is often a bottleneck in
 336 real-world BCI applications. Furthermore, the architecture’s rapid convergence and susceptibility
 337 to overfitting emphasize the need for further research into regularization techniques and adaptive
 338 training strategies specific to hypernetwork-based models. Looking forward, the findings suggest
 339 several key avenues for future exploration. This work sets the stage for more scalable, adaptive, and
 340 personalized BCIs, bridging the gap between laboratory research and practical, everyday use.

341

342 **REFERENCES**

343

344 Brendan Z. Allison and Christa Neuper. *Could Anyone Use a BCI?*, pp. 35–54. Springer London,
 345 London, 2010. ISBN 978-1-84996-272-8. doi: 10.1007/978-1-84996-272-8_3. URL https://doi.org/10.1007/978-1-84996-272-8_3.

347 L. M. Alonso-Valerdi and V. R. Mercado-García. Updating bci paradigms: Why to design in terms
 348 of the user? In *2021 10th International IEEE/EMBS Conference on Neural Engineering (NER)*,
 349 pp. 710–713, 2021. doi: 10.1109/NER49283.2021.9441337.

351 Bruno Aristimunha, Igor Carrara, Pierre Guetschel, Sara Sedlar, Pedro Rodrigues, Jan Sosulski,
 352 Divyesh Narayanan, Erik Bjareholt, Barthelemy Quentin, Robin Tibor Schirrmeister, Emmanuel
 353 Kalunga, Ludovic Darmet, Cattan Gregoire, Ali Abdul Hussain, Ramiro Gatti, Vladislav Gon-
 354 charenko, Jordy Thielen, Thomas Moreau, Yannick Roy, Vinay Jayaram, Alexandre Barachant,
 355 and Sylvain Chevallier. Mother of all BCI Benchmarks, 2023. URL <https://github.com/NeuroTechX/moabb>.

357 Suzanna Becker, Kiret Dhindsa, Leila Mousapour, and Yar Al Dabagh. Bci illiteracy: it’s us, not
 358 them. optimizing bcis for individual brains. In *2022 10th International Winter Conference on*
 359 *Brain-Computer Interface (BCI)*, pp. 1–3. IEEE, 2022.

361 Benjamin Blankertz, Claudia Sannelli, Sebastian Halder, Eva M Hammer, Andrea Kübler, Klaus-
 362 Robert Müller, Gabriel Curio, and Thorsten Dickhaus. Neurophysiological predictor of smr-based
 363 bci performance. *Neuroimage*, 51(4):1303–1309, 2010.

364 Clemens Brunner, Robert Leeb, Gernot Müller-Putz, Alois Schlögl, and Gert Pfurtscheller. Bci com-
 365 petition 2008–graz data set a. *Institute for knowledge discovery (laboratory of brain-computer*
 366 *interfaces), Graz University of Technology*, 16:1–6, 2008.

368 Aline Roc Pauline Dreyer Camille Jeunet Camille Benaroch, Maria Sayu Yamamoto and Fabien
 369 Lotte. When should mi-bci feature optimization include prior knowledge, and which one?
 370 *Brain-Computer Interfaces*, 9(2):115–128, 2022. doi: 10.1080/2326263X.2022.2033073. URL
 371 <https://doi.org/10.1080/2326263X.2022.2033073>.

372 Yuqi Chen, Kan Ren, Kaitao Song, Yansen Wang, Yifan Wang, Dongsheng Li, and Lili Qiu. Eeg-
 373 former: Towards transferable and interpretable large-scale eeg foundation model. *arXiv preprint*
 374 *arXiv:2401.10278*, 2024.

376 Ga-Young Choi, Soo-In Choi, and Han-Jeong Hwang. Individual identification based on resting-
 377 state eeg. In *2018 6th International conference on brain-computer interface (BCI)*, pp. 1–4.
 IEEE, 2018.

- 378 Pauline Dreyer, Aline Roc, Léa Pillette, Sébastien Rimbert, and Fabien Lotte. A large eeg database
 379 with users' profile information for motor imagery brain-computer interface research. *Scientific*
 380 *Data*, 10(1):580, 2023.
- 381
- 382 Matteo Ferrante, Tommaso Boccato, and Nicola Toschi. Towards neural foundation models for
 383 vision: Aligning eeg, meg and fmri representations to perform decoding, encoding and modality
 384 conversion. In *ICLR 2024 Workshop on Representational Alignment*, 2024.
- 385 Alexandre Gramfort, Martin Luessi, Eric Larson, Denis A. Engemann, Daniel Strohmeier, Christian
 386 Brodbeck, Roman Goj, Mainak Jas, Teon Brooks, Lauri Parkkonen, and Matti S. Hämäläinen.
 387 MEG and EEG data analysis with MNE-Python. *Frontiers in Neuroscience*, 7(267):1–13, 2013.
 388 doi: 10.3389/fnins.2013.00267.
- 389
- 390 David Ha, Andrew M. Dai, and Quoc V. Le. Hypernetworks. In *International Conference on Learning Representations*, 2017. URL <https://openreview.net/forum?id=rkpACellx>.
- 391
- 392 Khondoker Murad Hossain, Md. Ariful Islam, Shahera Hossain, Anton Nijholt, and Md Atiqur Rah-
 393 man Ahad. Status of deep learning for eeg-based brain–computer interface applica-
 394 tions. *Frontiers in Computational Neuroscience*, 16, 2023. ISSN 1662-5188. doi:
 395 10.3389/fncom.2022.1006763. URL <https://www.frontiersin.org/journals/computational-neuroscience/articles/10.3389/fncom.2022.1006763>.
- 396
- 397 Reinmar Kobler, Jun-ichiro Hirayama, Qibin Zhao, and Motoaki Kawanabe. Spd domain-specific
 398 batch normalization to crack interpretable unsupervised domain adaptation in eeg. *Advances in*
 399 *Neural Information Processing Systems*, 35:6219–6235, 2022.
- 400
- 401 Jean-Philippe Lachaux, Eugenio Rodriguez, Jacques Martinerie, and Francisco J Varela. Measuring
 402 phase synchrony in brain signals. *Human brain mapping*, 8(4):194–208, 1999.
- 403
- 404 Vernon J Lawhern, Amelia J Solon, Nicholas R Waytowich, Stephen M Gordon, Chou P Hung, and
 405 Brent J Lance. Eegnet: a compact convolutional neural network for eeg-based brain–computer
 406 interfaces. *Journal of neural engineering*, 15(5):056013, 2018.
- 407
- 408 Blu Wang Ma, Minett. Resting state eeg-based biometrics for individual identification using con-
 409 convolutional neural networks. 2015. URL <https://ieeexplore.ieee.org/abstract/document/7318985/keywords#keywords>.
- 410
- 411 Aarthy Nagarajan, Neethu Robinson, Kai Keng Ang, Karen Sui Geok Chua, Effie Chew, and Cuntai
 412 Guan. Transferring a deep learning model from healthy subjects to stroke patients in a motor im-
 413 agery brain–computer interface. *Journal of Neural Engineering*, 21(1):016007, jan 2024. doi: 10.
 414 1088/1741-2552/ad152f. URL <https://dx.doi.org/10.1088/1741-2552/ad152f>.
- 415
- 416 Yue-Ting Pan, Jing-Lun Chou, and Chun-Shu Wei. Matt: A manifold attention network for eeg
 417 decoding. *Advances in Neural Information Processing Systems*, 35:31116–31129, 2022.
- 418
- 419 Simanto Saha and Mathias Baumert. Intra-and inter-subject variability in eeg-based sensorimotor
 420 brain computer interface: a review. *Frontiers in computational neuroscience*, 13:87, 2020.
- 421
- 422 Gerwin Schalk, Peter Brunner, Brendan Z Allison, Surjo R Soekadar, Cuntai Guan, Tim Denison,
 423 Jörn Rickert, and Kai J Miller. Translation of neurotechnologies. *Nature Reviews Bioengineering*,
 424 pp. 1–16, 2024.
- 425
- 426 Catherine Tallon-Baudry, Olivier Bertrand, Claude Delpuech, and Jacques Pernier. Oscillatory γ -
 427 band (30–70 hz) activity induced by a visual search task in humans. *Journal of Neuroscience*, 17
 428 (2):722–734, 1997.
- 429
- 430 Margaret C Thompson. Critiquing the concept of bci illiteracy. *Science and engineering ethics*, 25
 431 (4):1217–1233, 2019.
- 432
- 433 Navneet Tibrewal, Nikki Leeuwis, and Maryam Alimardani. Classification of motor imagery eeg
 434 using deep learning increases performance in inefficient bci users. *PLOS ONE*, 17(7):1–18, 07
 435 2022. doi: 10.1371/journal.pone.0268880. URL <https://doi.org/10.1371/journal.pone.0268880>.

432 David Trocellier, Bernard N’Kaoua, and Fabien Lotte. Validating neurophysiological predictors of
 433 bci performance on a large open source dataset. In *9th Graz Brain-Computer Interface Conference*
 434 *2024-GBCIC2024*, 2024.

435 Tanaka Uchikawa Tshukahara, Anzai. A design of eegnet-based inference processor for pattern
 436 recognition of eeg using fpga. *Electronics and Communications in Japan*, 1:53–64, 2021. ISSN
 437 1942-9533.

438 Eidan Tzdaka, Camille Benaroch, Camille Jeunet, and Fabien Lotte. Assessing the relevance of
 439 neurophysiological patterns to predict motor imagery-based bci users’ performance. In *2020*
 440 *IEEE International Conference on Systems, Man, and Cybernetics (SMC)*, pp. 2490–2495, 2020.
 441 doi: 10.1109/SMC42975.2020.9283307.

442 Min Wang, Heba El-Fiqi, Jiankun Hu, and Hussein A Abbass. Convolutional neural networks using
 443 dynamic functional connectivity for eeg-based person identification in diverse human states. *IEEE*
 444 *Transactions on Information Forensics and Security*, 14(12):3259–3272, 2019.

445 Fangzhou Xu, Yunjing Miao, Yanan Sun, Dongju Guo, Jiali Xu, Yuandong Wang, Jincheng Li,
 446 Han Li, Gege Dong, Fenqi Rong, et al. A transfer learning framework based on motor imagery
 447 rehabilitation for stroke. *Scientific Reports*, 11(1):19783, 2021.

448 Zhi Zhang, Sheng hua Zhong, and Yan Liu. TorchEEGEMO: A deep learning toolbox towards
 449 EEG-based emotion recognition. *Expert Systems with Applications*, pp. 123550, 2024. ISSN
 450 0957-4174.

453 A APPENDIX

454 We plan to make our code publicly available on acceptance to ensure reproducibility and facilitate
 455 further research.

456 A.1 LEAVE-N-OUT ANALYSIS FOR DREYER ET AL. 2023 DATASET

457 For the Leave-N-out (with N=8,16 and 32) strategy to test the HyperEEGNet performance com-
 458 pared to EEGNet, the “acquisition runs” from randomly selected (42-N) participants were used for
 459 training. 20% split is used as a validation set to select the best model. Performance evaluation with
 460 accuracy metrics is performed using data from the N participants for the “online” runs to eval-
 461 uate HyperEEGNet compared to EEGNet. Analysis of such 100 random combinations reports the
 462 mean accuracy and standard deviation in Table 4. Non-parametric statistical tests (Wilcoxon Signed
 463 Rank Test) recorded a statistically significant increase ($p < 0.005$ for all N) in the performance using
 464 HyperEEGNet compared to EEGNet.

465 Number of 466 participants in 467 test set (N)	468 HyperNet 469 + EEGNet (%)	470 EEGNet (%)
471 8	472 84.10 ± 02.11	473 83.87 ± 02.10
474 16	475 84.86 ± 01.02	476 83.94 ± 00.97
477 32	478 76.47 ± 02.00	479 73.45 ± 02.61

480 Table 4: Mean accuracy with standard deviation (SD) across 100 combinations of cross-user condi-
 481 tion on Dreyer et al. 2023 dataset with Leave N Subject Out strategy.

482 A.2 SESSION-WISE ANALYSIS FOR BCI IV IIa DATASET

483 For the BCI IV IIa dataset, since there are just 9 participants, we use the Leave one subject out
 484 (LOSO) a strategy where, across nine folds, each participant’s performance is evaluated while train-
 485 ing on the first session data from 8 participants. Analysis reports the mean accuracy and standard
 486 deviation in Table 5 Accuracy metrics are evaluated on the second session’s data of each participant
 487 left out during training. Non-parametric statistical tests (Wilcoxon Signed Rank Test) recorded a sta-
 488 tistically significant decrease ($p < 0.05$ for all N) in the performance using HyperEEGNet compared
 489 to EEGNet.

	Participant ID	HyperNet + EEGNet (%)	EEGNet (%)
488	1	60.42	75.00
489	2	50.69	59.72
490	3	59.03	90.97
491	4	59.72	62.50
492	5	57.63	59.72
493	6	63.88	68.05
494	7	56.94	51.38
495	8	74.30	95.83
496	9	59.02	70.13
497	Mean ± SD	60.19 ± 06.35	70.37 ± 14.78

498 Table 5: Mean accuracy with standard deviation (SD) using test session for cross-user condition on
499 BCI Competition IV IIa Dataset with Leave One Subject Out (LOSO) strategy.

501 A.3 SESSION-WISE ANALYSIS FOR BCI IV IIb DATASET

503 BCI IV IIb dataset is different from BCI IV IIa since the number of EEG channels used for data
504 recording are 3 compared to 22. Since there are just 9 participants, we use the Leave one subject out
505 (LOSO) a strategy where, across nine folds, each participant's performance is evaluated while training
506 on the first session data from 8 participants. Analysis reports the mean accuracy and standard
507 deviation in Table 6 Accuracy metrics are evaluated on the second session's data of each participant
508 left out during training. Non-parametric statistical tests (Wilcoxon Signed Rank Test) recorded a sta-
509 tistically significant decrease ($p < 0.05$ for all N) in the performance using HyperEEGNet compared
510 to EEGNet.

	Participant ID	HyperNet + EEGNet (%)	EEGNet (%)
513	1	63.12	75.31
514	2	49.64	57.50
515	3	51.87	54.06
516	4	83.12	86.25
517	5	57.50	78.12
518	6	54.06	79.06
519	7	56.87	72.18
520	8	85.00	79.37
521	9	60.62	88.75
522	Mean ± SD	62.42 ± 12.94	74.51 ± 11.78

523 Table 6: Mean accuracy with standard deviation (SD) using test session for cross-user condition on
524 BCI Competition IV IIb Dataset with Leave One Subject Out (LOSO) strategy.